Resonance Phase Transistor – Concepts and Perspectives

H. Jorke, M. Schäfer*, J.-F. Luy

DaimlerChrysler Research Center Ulm
Wilhelm-Runge-Str. 11, 89081 Ulm, Germany

***CADwalk Design & Simulation**
Stegäckerstrasse 7, 89604 Allmendingen, Germany

Abstract **- Two concepts of creating a negative output resistance three-terminal device by shifting the collector current phase in excess of** p **are investigated. With the concept of counter-phase injection, which exploits resonant tunneling, the three-terminal device shows a negative output resistance in the whole frequency range up to a cut-off frequency. In contrast, with the concept of delayed injection using a more conventional bipolar transistor structure, the negative output resistance is found to be confined to a frequency band. In both transistor types, the magnitude of the negative output resistances are comparable. In addition, by a numerical simulation, high current effects are investigated in the delayed injection transistor.**

Introduction

Fabrication of oscillator circuits with transistors commonly uses the amplification character of these active elements in a way, by means of embedding them into an appropriate circuit network, that there is a reference plane characterized by a negative resistance. This conventional procedure of power generation is limited to frequencies below the maximum frequency of oscillation. Although by continuously decreasing structural dimensions, cut-off frequencies have been impressively raised there are limits existing, both for technological and physical reasons, that make it questionable if oscillators can be fabricated in silicon based circuits at frequencies well above 100 GHz.

A new way to overcome this limitations is opened by the principle of resonance phase amplification that was previously discussed in reference [1]. In this scheme, by increasing the collector current phase angle beyond a value of π, power generation is accomplished by creating a negative resistance reference plane immediately at the output of the two-port device.

Considering the simplified microwave equivalent circuit as depicted in Fig. 1, the common emitter output resistance of this two-port device can be expressed as

$$R_{22} = \{|\alpha_E\, \alpha_B\, \alpha_C| / \omega C_{BC}\} \sin(\phi + \theta/2) + R_E\, \mathrm{Re}(\alpha_E) \qquad (1)$$

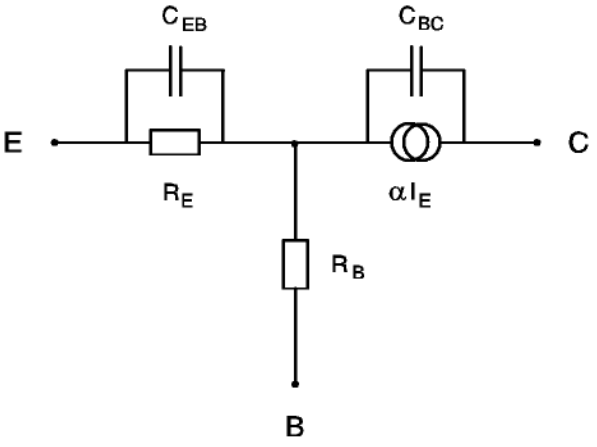

Fig. 1 Simplified equivalent circuit of a bipolar transistor.

This formula reveals that, next to the phase delays of injection ϕ and collector transit θ, the total of the transport factor $\alpha = \alpha_E \alpha_B \alpha_C$ is of central importance to the magnitude of the negative output resistance R_{22}. Following Eq. 1 the phase angle condition to get optimum negative resistance values reads

$$\phi + \theta/2 = 3\pi/2 \qquad (2)$$

In principle, this condition may be fulfilled either by choosing sufficiently large values of ϕ or θ. However, the collector transport factor α_C becomes zero at $\theta/2 = \pi$ (see below). Thus, the task is to attain injection angles θ significantly in excess of $\pi/2$ at, simultaneously, sufficiently high values of α_E and α_B. Two ways, to our knowledge, exist to that aim:

1) *Delayed injection using a thick base layer*. This concept has been formerly discussed by several authors [2 – 6]. To increase the total of α_B in this case, diffusive motion of minority carriers through the base is enhanced in the forward direction by drift fields [5] due to either compositional gradients or doping gradients (or both). If carriers are monoenergetically injected into the base layer and there is no dissipation of energy (ballistic transport), modulation of minority carrier waves is preserved during the base transit. This ideal situation corresponds to $\alpha_B = 1$, the coherent transport [6].

2) *Counter-phase injection into the collector using a quantum-well base injector that exploits resonant tunneling* (see Fig. 2 and 3). In this case, the injection angle approaches $\phi = 3\pi/2$, which makes an additional delay in the collector dispensable (see Eq. 1). However, with very small base-collector depletion width, the base-collector capacitance C_{BC} becomes large, reducing the output resistance again (Eq. 1). This means there is an optimum in the range $0 < \theta < \pi/2$.

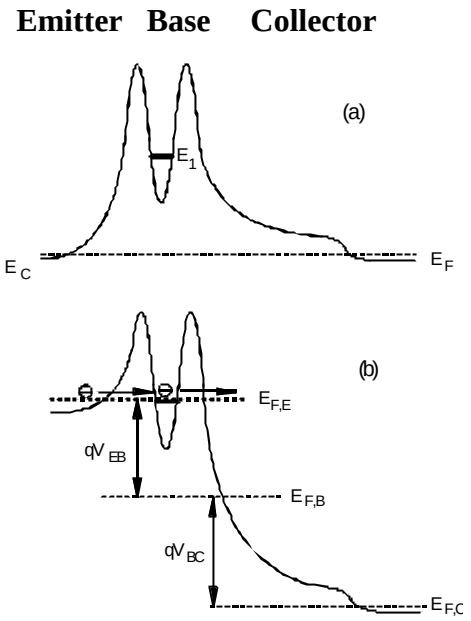

Fig. 2 CB diagram of a double-barrier base bipolar transistor (a) in equilibrium and (b) under emitter-base forward bias condition.

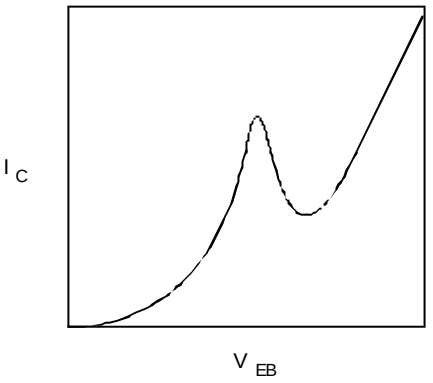

Fig. 3 Collector current vs. emitter-base bias of a double-barrier base bipolar transistor.

High frequency properties of the counter-phase injection resonance-phase transistor (RPT)

Considering the simplified equivalent circuit in Fig. 1, the common emitter impedance matrix is given by

$$Z = \begin{bmatrix} R_B + R_E a_E & R_E a_E \\ \dfrac{a}{iwC_{BC}} + R_E a_E & \dfrac{1-a}{iwC_{BC}} + R_E a_E \end{bmatrix} \qquad (3)$$

which implies that for R_{22} = Re Z_{22} the output resistance is

$$R_{22} = - \mathrm{Im}(\alpha_E \alpha_B \alpha_C)/\omega C_{BC} + R_E \mathrm{Re}(\alpha_E) \qquad (4)$$

The individual transport factors are written for the counter-phase injection RPT as follows

$$a_E = \frac{1}{1 + iwR_E C_{EB}} \qquad (5\ a)$$

$$a_B = 1 \qquad (5\ b)$$

$$a_C = \frac{1 - e^{-iq}}{iq} \qquad (5\ c)$$

with $\theta = \omega\tau_C$ where τ_C = collector transit time (space charge width over saturation velocity). Note that the emitter resistance R_E - depending on the point of operation (see Fig. 3) - is either positive in sign for in-phase injection or negative in sign for counter-phase injection. Fig. 4 and Fig. 5 show phase trajectories of the emitter transport factor (presuming a negative sign for the emitter resistance) and the collector transport factor, respectively.

Inserting Eq. 5 a – c into Eq. 4 we get the output resistance R_{22} as depicted in Fig. 6. Results show that the device amplifies incoming signals in the whole frequency range up to a cut-off frequency that depends on the collector width. The dependence of the output resistance on the collector width is shown in Fig. 7. At very small collector widths, the output resistance increases with growing collector width due to the decrease of the base-collector capacitance. At large collector widths the output resistance decreases again, which is caused here by the decrease of the collector transport factor. From this analysis, at operation frequencies in the V band (50 – 75 GHz), optimum values of the output resistance will be obtained at about a 300 nm collector width.

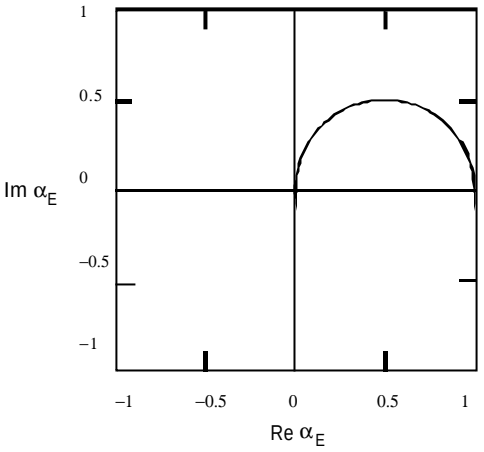

Fig. 4 Phase trajectory of the emitter transport factor at a negative emitter resistance.

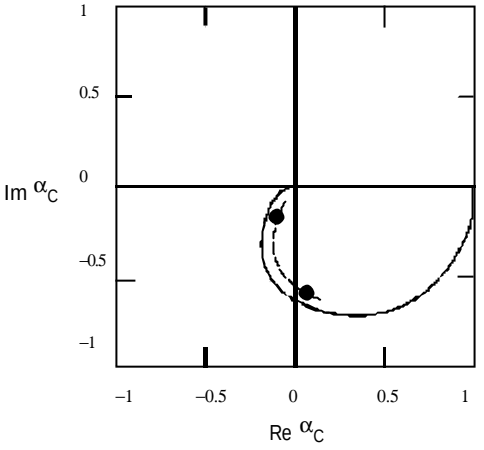

Fig. 5 Phase trajectory of the collector transport factor.

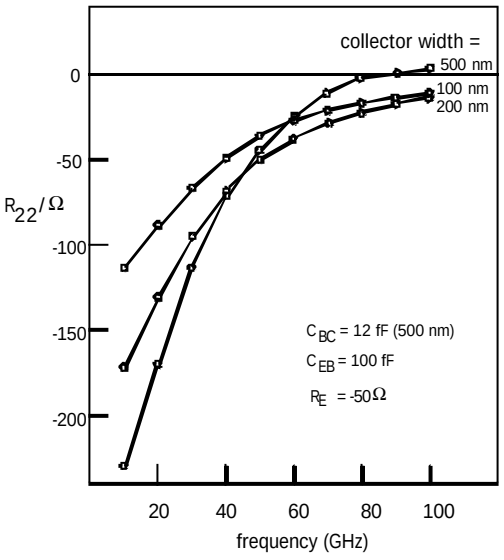

Fig. 6 Output resistance vs. frequency of the counter-phase injection RPT. E-B and B-C capacitances were assessed from space-charge widths. The value of R_E follows reference [7].

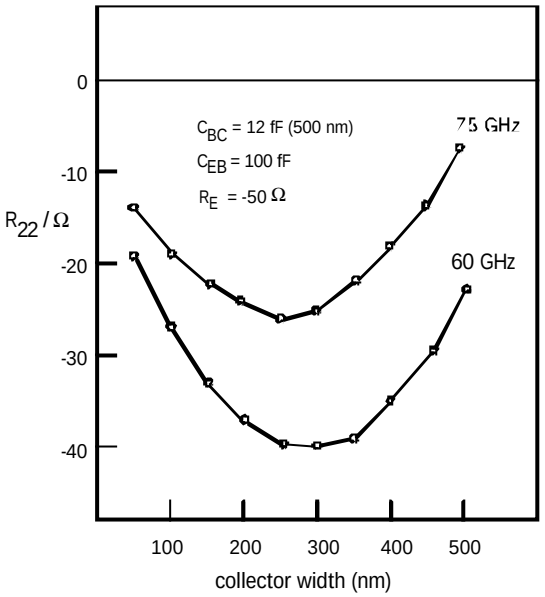

Fig. 7 Output resistance vs. collector width of the counter-phase injection RPT.

High frequency properties of the delayed injection resonance-phase transistor (RPT)

This RPT concept makes use of finite transit times carriers need to cross the base and the collector of a bipolar transistor. Delays by these transit times are adjusted in a way that the phase angle condition Eq. 2 is fulfilled.

In standard high frequency bipolar transistors that are optimized regarding small base transit times, the injection angle $\phi = \phi_E + \phi_B$ is dominated by the phase delay ϕ_E due to the emitter-base capacitance. In this case, the injection angle approaches, at high frequencies, the capacitive phase delay $\phi = \pi/2$. So, to satisfy the RPT phase angle condition Eq. 2, the collector width has to be designed such that $\theta = 2\pi$. This particular combination of delays for injection ϕ and collector transit θ essentially suffers from the zero of the collector transport factor at this transit angle (see Eq. 5 c). Correspondingly, previous investigations [4, 8] showed that negative resistances due to transit time effects in conventional bipolar transistors are readily swamped by the device parasitics. Thus, in order to optimize the bipolar transistor regarding resonance phase amplification (i.e. negative output resistance) both emitter-base and collector regions need to be properly configured.

The impedance matrix Z and the output resistance $R_{22} = \mathrm{Re}\, Z_{22}$ for the simplified equivalent circuit (Fig. 1) are, like the counter-phase injection case, given by Eq. 3 and Eq. 4 , respectively. The individual transport factors , however, read in the present case

$$a_E = \frac{1}{1 + iwR_E C_{EB}} \qquad (6\ a)$$

$$a_B = \frac{e^r}{\cosh(l) + \frac{r}{l}\sinh(l)} \qquad (6\ b)$$

$$a_C = \frac{1 - e^{-q}}{iq} \qquad (6\ c)$$

where the emitter transport factor is determined by the (always positive) emitter resistance $R_E = kT/qI_C$ and the emitter-base capacitance C_{BC}. The corresponding phase trajectory is shown in Fig. 8.

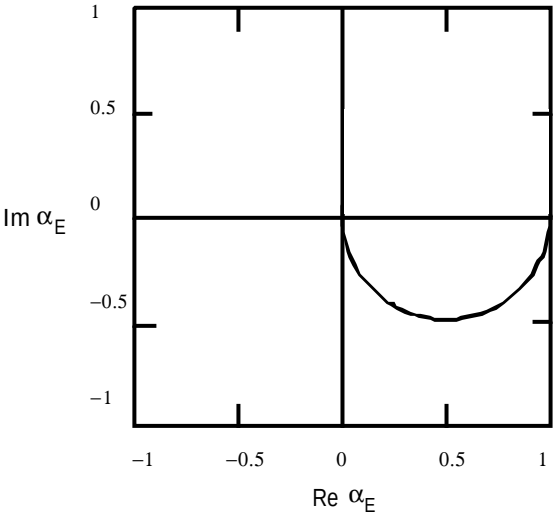

Fig. 8 Phase trajectory of the emitter factor in a delayed injection RPT.

The base transport factor α_B (Eq. 6 b) takes into account the presence of a drift field due to a compositional grading of the base layer. Parameters in this expression are

$$r = \Delta E_g / 2kT \qquad (7\ a)$$

$$l = (r^2 + 2(iv + \frac{1}{t_n})t_B)^{1/2} \qquad (7\ b)$$

with ΔE_g = band gap change within the base, W_B base width, $\tau_B = W_B^2/2D_n$ and τ_n = recombination lifetime of electrons in the base. For the flat base (r = 0) and vanishing recombination ($\tau_n^{-1} = 0$) we get [9]

$$a_B = \frac{1}{\cosh\left[\sqrt{2iv\,t_B}\right]} \qquad (8)$$

Phase trajectories of α_B corresponding to r = 0 (flat base) and r = 3 are depicted in Fig. 9. The latter case is related to a compositional grading with a band gap change of ΔE_g = 150 meV. This comparitive plot reveals that, at equal phase angles, the magnitude of the base transport factor is significantly enhanced by the drift field in the base.

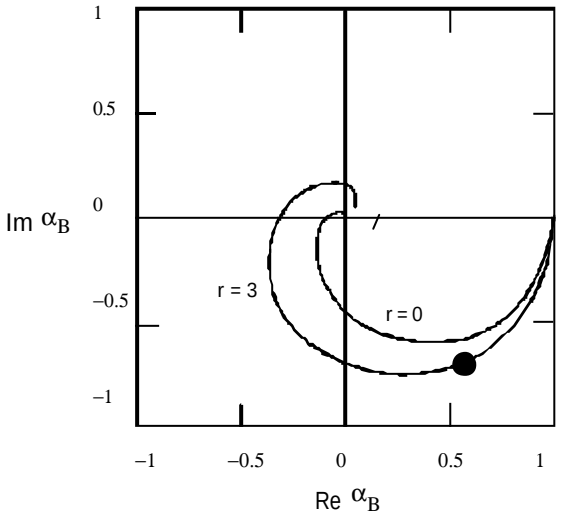

Fig. 9 Phase trajectory of the base transport factor in a delayed injection RPT for a flat base (r = 0) and for a graded base (r = 3).

Inserting Eq. 6 a – c into Eq. 4, we get the output resistance R_{22} as depicted in Fig. 10. In contrast to the counter-phase injection device (Fig. 6), the negative resistance is confined to a frequency band.

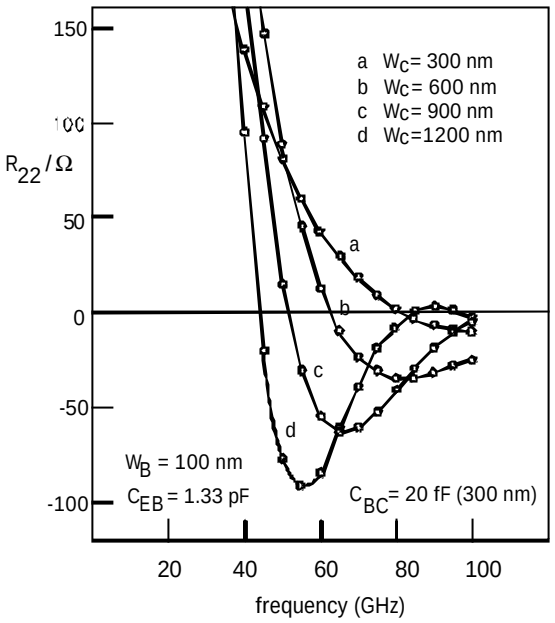

Fig. 10 R_{22} vs. frequency of the delayed injection RPT with r = 3, R_E = 2.5 Ω, D_n = 5 cm^2/s. Capacitances are related to an emitter size of 1 x 10 μm^2.

Next, we consider a more realistic equivalent circuit (see Fig. 11) that differs essentially by the feedback capacitance C_{fb} from the more simple equivalent circuit shown in Fig. 1

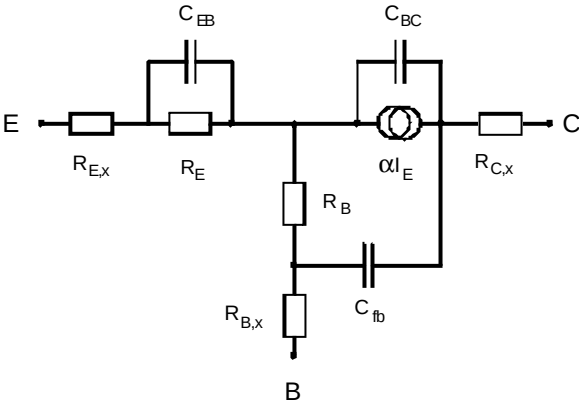

Fig. 11 Extended equivalent circuit of the bipolar transistor that considers the feed-back capacitance C_{fb}.

Results regarding the output resistance are presented in Fig. 12. As before, there are bands of negative output resistance where the impedance level, by virtue of the feedback capacitance, is somewhat reduced, as we expected.

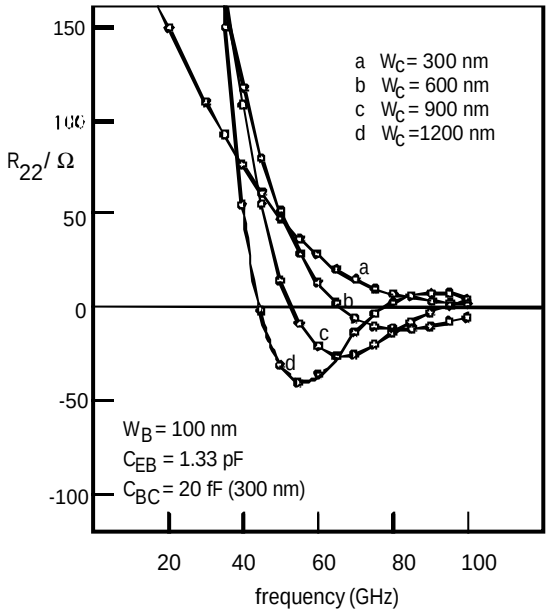

Fig. 12 R_{22} vs. frequency of the delayed injection RPT using the extended equivalent circuit model shown in Fig. 11.

On the basis of this more realistic equivalent circuit, we modeled the dependency of R_{22} on the collector width at a fixed operation frequency of f = 60 GHz and different widths of the base while keeping the band gap change in the graded base constant (r = 3). Results presented in Fig. 13 show an optimum collector width for each base width, which behaves reciprocally to the width of the base. With respect to the height of the impedance level (total of R_{22} at the optimum collector width), results reveal, that there is an optimum trade-off between base delay and collector delay. The highest impedance level, for the target frequency of f = 60 GHz, is observed at a base width of about 100 nm and a collector width of 1100 nm.

Analogous results at an operation frequency of f = 75 GHz are shown in Fig. 14. At this higher frequency the optimum trade-off is found to be between a 75 nm and 100 nm base width and at about an 800 nm collector width.

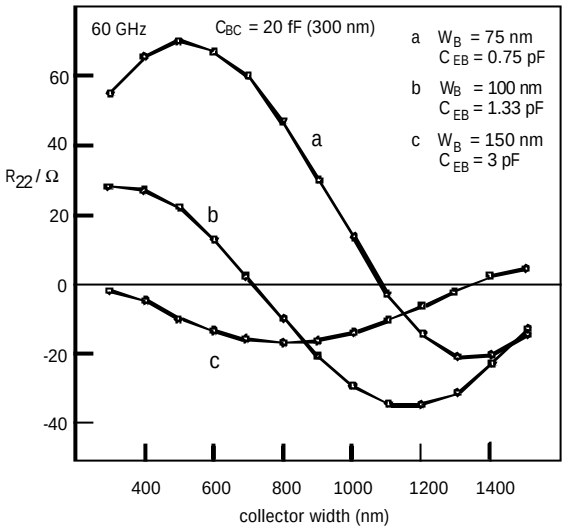

Fig. 13 R_{22} vs. collector width for the delayed injection RPT with graded base (r = 3) at three different base widths (75, 100, 150 nm) at a target frequency of f = 60 GHz.

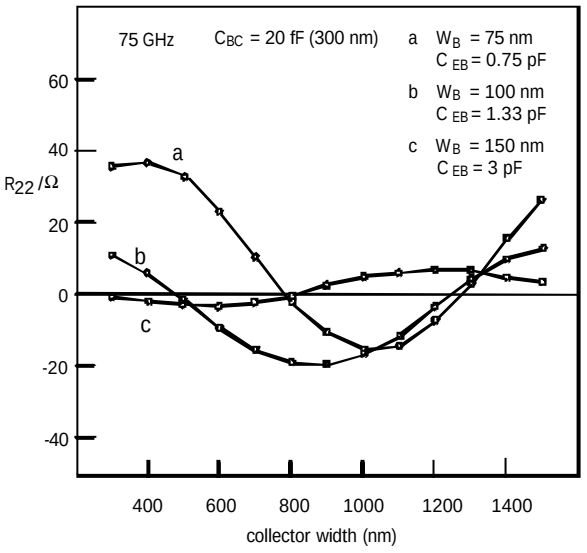

Fig. 14 R_{22} vs. collector width for the delayed injection RPT with graded base (r = 3) at three different base widths (75, 100, 150 nm) at a target frequency of f = 75 GHz.

In order to check results discussed so far, which are obtained from analytical models of transport factors (Eq. 6 a - c), numerical simulations were carried out considering the Si/SiGe heterojunction system. This part of the work is based on the 2D simulator ATLAS from SILVACO. This simulator characterizes the resonance phase transistor (RPT) on a physical level by solving a coupled set of six differential equations considering phenomena such as recombination, bandgap narrowing and field and doping dependencies of majority and minority carrier mobilities.

Transport factors in different areas of the device (emitter, base, collector) are attained by a dynamic model based on a transient analysis. Cut lines are placed into different places of the inner structure of the transistor (at the transitions emitter-base, base-collector and collector-subcollector), which allows for an individual assessment of transport factors, which are key elements, by integrating current densities along these lines (see Fig. 15). In this way, we are getting information both regarding the modulation decrease of a carrier wave crossing the respective layer and the corresponding phase delay.

The aim of this work was not only to verify the analytical model but also to investigate high current effects that are not accessible by the analytical model.

At relatively small collector currents (below 2.5 mA with an emitter area of 1x10 μm^2) the numerical simulation largely corroborates the analytical modeling. This is shown in Fig. 5 and Fig. 9, where the dots present numerical results. However, with increasing current density, we found a sudden breakdown in the modulation of carrier waves. This breakdown is located at the base-collector interface and is correlated to the onset of the Kirk-effect (base push-out). Fig. 16 shows this breakdown that causes a drop of the transport factor from about α = 0.1 at collector currents below 2.5 mA to α = 0.0025 at a 5 mA collector current (1 x 10 μm^2 emitter size, respectively).

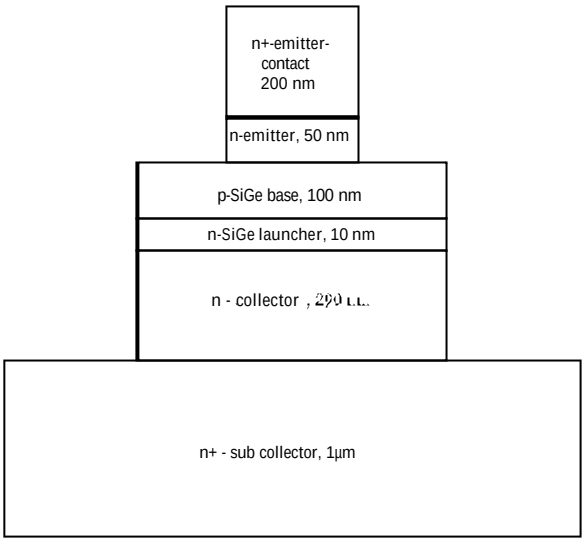

Fig. 15: 2D structure of a RPT considered for numerical AC simulation

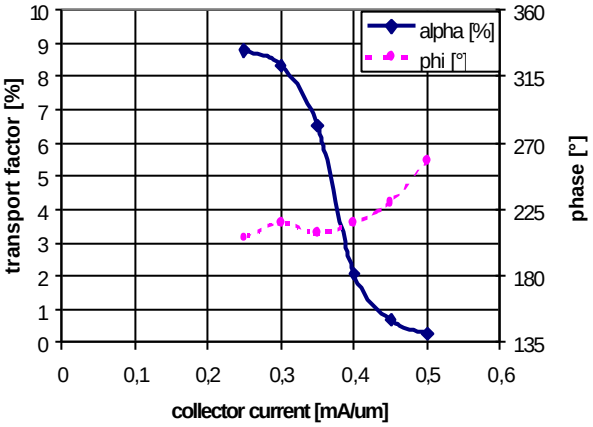

Fig. 16: Transport factor α (solid line) and total phase angle (dashed line) vs. collector current density for the delayed injection RPT.

References

[1] H. Jorke, J. Weller, J.-F. Luy, "Resonance phase amplification – a concept for operating Si based devices at mm wave frequencies ?", in "Future Trends in Microelectronics: The Road Ahead", Eds. S. Luryi, J. Xu, A. Zaslavsky, John Wiley & Sons, 1999

[2] G.T. Wright, “Small-signal theory of the transistor transit-time oscillator (translator)", Solid State Electronics 22, 399 (1979)

[3] N. Dagli, “Physical origin of the negative output resistance of heterojunction bipolar transistors“, IEEE Electron Device Lett. 9. 113 (1988)

[4] S. Tiwari, “Frequency dependence of the unilateral gain in bipolar transistors", IEEE Electron Device Letters 10, 574 (1989)

[5] A.A. Grinberg, S. Luryi, “Coherent transistor", IEEE Transactions on Electron Devices 40, 1512 (1993)

[6] S. Luryi, A.A. Grinberg, V.B. Gorfinkel, “Heterostructure bipolar transistor with enhanced forward diffusion of minority carriers", Appl. Phys. Lett. 63, 1537 (1993)

[7] G.M. Cohen, D. Ritter, “Microwave performance of $Ga_xIn_{1-x}P/Ga_{0.47}In_{0.53}As$ resonant tunneling diodes", Electronic Letters 34, 1267 (1998)

[8] S. Luryi, “Ultrafast Operation of heterostructure bipolar transistors resulting from coherent base transport of minority carriers", Proceedings Int. Semicond. Dev. Res. Symp. 93, Charlotteville, 59 (1993)

[9] P.M. Asbeck, “Bipolar Transistors“, in „Modern Semiconductor Device Physics“, S.M. Sze (Herausg.), John Wiley & Sons (1998), S. 70